Optical nuclear magnetic resonance: theory, simulation, and animation

Myron W. Evans* and Chris R. Pelkie

Center for Theory and Simulation in Science and Engineering, Cornell University, Ithaca, New York 14853-3801

Received September 10, 1990; revised manuscript received October 21, 1991

The theory of optical nuclear magnetic resonance (NMR) is introduced and developed with supercomputer simulation and animation. A powerful, circularly polarized pulse of laser radiation magnetizes an ensemble of atoms and molecules through the conjugate product of nonlinear optical theory. This magnetization is shown theoretically to result in nonlinear optical Zeeman splitting—the optical Zeeman effect—mediated by the orbital and the spin electronic and nuclear quantum numbers through a new fundamental property, the gyroptic ratio. When a circularly polarized laser is used in a conventional NMR spectrometer, the spectrum is split by Landé coupling, leading to a new analytical technique, optical NMR. This development is potentially of widespread interest. The interaction of a circularly polarized laser with optically active (chiral, or handed) molecules leads to electric polarization, and the statistical dynamical origins of this effect are simulated and animated on the IBM supercomputer of the Cornell Theory Center. Scientific visualization reveals the nature of orientational cross correlations induced by the circularly polarized laser; a novel time-lapse method is used to relate the statistical and actual (motion) correlations. These correlations yield the torque effect of the circularly polarized laser, which imparts net angular momentum whose motion reversal and parity inversion symmetries are the same as those of magnetization.

1. INTRODUCTION

After Faraday[1] in 1846 discovered the occurrence in lead borate glass of circular birefringence caused by static magnetic flux density **B**, Zeeman[2] in 1896 reported a broadening of the principal doublet of sodium vapor placed between the poles of a powerful electromagnet. Quantum mechanics was used by Serber[3] in 1932 to show that the Zeeman effect is the A term of the quantum description of the Faraday effect, a finding that was reinforced theoretically by Buckingham and Stephens,[4] using dynamic molecular property tensors, in 1966. Magnetic electronic optical activity is described in these contemporary terms[5,6] by the imaginary part of the complex atomic or molecular polarizability $i\alpha''_{ij}$, which is an antisymmetric second-rank polar tensor, negative with respect to motion reversal T and positive in parity inversion P. The quantity is conveniently referred to below as angular polarizability, with general orbital and spin components. That $i\alpha''_{ij}$ is negative to T means[5] that it must be activated by a T-negative external influence so that it may mediate the Faraday and Zeeman effects. This influence is conventionally the applied **B**, which is a T-negative, P-positive axial vector from fundamental theory.[5]

Here we develop a simple quantum theory of the optical Faraday and Zeeman effects, using in place of **B** another activating influence, the conjugate product Π of a circularly polarized pump laser. The quantity Π is also an axial vector (or antisymmetric polar tensor) that is T negative and P positive and proportional to the square of the electric-field strength E_o (in volts per meter) of the pump laser. Π switches signs if the pump laser's circular polarity is switched from right to left and disappears if the pump laser is plane polarized or unpolarized. It is a purely imaginary quantity and forms a real scalar interaction Hamiltonian through the appropriate vector or tensor product with the angular polarizability axial vector $i\alpha''_i$, another purely imaginary quantity. This interaction Hamiltonian is developed in Section 2.

In 1963 Pershan[7] showed theoretically that a circularly polarized laser causes magnetization through the phenomenon of optical rectification, which was reviewed by Ward.[8] This has become known as the inverse Faraday effect and was demonstrated experimentally by van der Ziel *et al.*[9] and by Pershan *et al.*[10] in paramagnetic and diamagnetic materials, including several diamagnetic liquids.[10] The experimental demonstration consisted of inducing a small electric current with an induction coil, using the bulk magnetization caused by a pulse of circularly polarized giant ruby laser radiation; no spectral effects were reported in this pioneering demonstration. The theory was later developed by Atkins and Miller.[11] The inverse Faraday effect was reviewed by Shen[12] and by Wagnière,[13] and it can be thought of as the Faraday effect with **B** replaced by Π for a circularly polarized pump laser. The spectral consequences of the magnetization of the inverse Faraday effect are developed in this paper for the first time to our knowledge in terms of the angular polarizability and its quantization properties, which are shown to be those of angular momentum itself, properties that form a cornerstone of the quantum theory and pervade much of atomic and molecular spectroscopy. The angular polarizability is the analog of the magnetic dipole moment in the coventional Zeeman effect, which leads to a straightforward understanding of the inverse Faraday effect and its expected spectral manifestations.

Evans[14–16] recently demonstrated theoretically the existance of forward–backward birefringence, which is analogous to the Wagnière–Meier effect that is due to **B**,[17–21] and estimated the extent of circular birefringence in a Q-switched Nd:YAG laser,[14] this quantity being roughly 10^6 rad/m for a pulse delivering E_o of ~10,000 V/cm. This

0740-3224/92/071020-10$05.00

field strength is easily achievable in a small contemporary Nd:YAG laser, which can be simultaneously Q switched, focused, and circularly polarized. The realization that $\mathbf{B}$ can be replaced optically by Π recently led to the theoretical development of several related spectral effects, including Π-induced forward–backward birefringence,[14–16] Π-induced optical activity in scattered radiation,[22,23] Π-induced P-violating phenomena in spectra,[24–26] and Π-induced electronic and nuclear resonance (this paper), of potentially widespread analytical utility. Additionally, Evans and Wagnière[26] developed the theory of Π-induced electric polarization that is sustained only in chiral ensembles and can be observed in achiral ensembles only in the presence of parity nonconservation.

In Section 3 we provide a detailed analysis of one of these effects, the optical Zeeman effect, and use the fundamental symmetry of the angular polarizability and of the optical property Π to distinguish it carefully at the outset from the well-known effect described by Autler and Townes[27] and from the optical Autler–Townes effect,[28–33] which is also known as the ac, optical, or quadratic Stark effect. The latter has been observed experimentally on several occasions, for example, by using a sodium atomic beam and unpolarized dye lasers.[28] In Section 3 we show that the Autler–Townes effects are mediated by the P- and T-positive real part of the dynamic polarizability, which is a symmetric tensor with no rank-one axial vector equivalent and which consequently exists in the absence of a T-negative influence such as Π or $\mathbf{B}$. The Autler–Townes effects have none of the fundamentally interesting angular-momentum quantization properties of the optical Zeeman effect.

Section 4 is a theoretical development of the optical Zeeman effect[34,35] in terms of the angular-momentum quantum numbers of a diatomic molecule. We demonstrate theoretically the expected spectrum in a simple diatomic, for example, a diatomic molecular beam.

In the final sections we discuss the optimum experimental conditions for the observation of the optical Zeeman effect and its electronic and nuclear spin hyperfine structure, the optical equivalent of nuclear magnetic resonance (NMR) and electron spin (paramagnetic) resonance (ESR). These conditions have been simulated[26] and animated (this paper) at the Cornell Theory Center. Algorithms and techniques used in the simulation and visualization are briefly described in Section 5.

2. INTERACTION HAMILTONIAN OF THE OPTICAL ZEEMAN EFFECT

The interaction Hamiltonian is confined to a description to first order in Π of its interaction with the angular polarizability. The semiclassical theory[5] of an atom or a molecule in a radiation field is used for this purpose. Specifically, we refer to the dynamic multipole interaction Hamiltonian, Eq. (2.5.30) of Ref. 5, and develop it to a higher order[8,13,22] in the electric-field strength $\mathbf{E}$ and magnetic flux density $\mathbf{B}$ of the electromagnetic field. Barron and Gray[36] demonstrated in 1973 that the dynamic multipole interaction Hamiltonian is fundamental and general provided that the Lorentz gauge is chosen correctly. Evans[22] developed it to a higher order by using a double Taylor expansion in $\mathbf{E}$ and $\mathbf{B}$, which are in general complex quantities from the plane-wave solution of Maxwell's equations. Accordingly

$$\Delta H = -\mu_i E_i - m_i B_i - 1/2\,\alpha_{ij} E_i E_j - 1/2\,\alpha_{1ij} E_i B_j - 1/2\,\alpha_{2ij} B_i E_j - 1/2\,\alpha_{3ij} B_i B_j + \ldots, \tag{1}$$

where the molecular property tensors α_{ij}, α_{1ij}, and so on are also complex quantities. For the optical Zeeman Hamiltonian of this section we are specifically interested in the term

$$\Delta H_1 = -1/2\,\alpha_{ij} E_i E_j, \tag{2}$$

where

$$\alpha_{ij} \equiv \alpha'_{ij} - i\alpha''_{ij} \tag{3}$$

is the complex electronic dynamical polarizability and where the electric-field terms are, in general,

$$\begin{aligned}
\mathbf{E}_-^{(L)} &= E_o(\mathbf{i} + i\mathbf{j})\exp(-i\Theta_L),\\
\mathbf{E}_-^{(R)} &= E_o(\mathbf{i} - i\mathbf{j})\exp(-i\Theta_R),\\
\mathbf{E}_+^{(L)} &= E_o(\mathbf{i} - i\mathbf{j})\exp(i\Theta_L),\\
\mathbf{E}_+^{(R)} &= E_o(\mathbf{i} + i\mathbf{j})\exp(i\Theta_R).
\end{aligned} \tag{4}$$

These plane-wave solutions of Maxwell's equation denote right (R) or left (L) circular polarization, and $+$ and $-$ complex conjugates.[8,13–16,22–26] The phases are, as usual,

$$\Theta_L = \omega t - \mathbf{K}_L \cdot \mathbf{r}, \qquad \Theta_R = \omega t - \mathbf{K}_R \cdot \mathbf{r}, \tag{5}$$

where ω is the angular frequency of the electromagnetic field in radians per second, $\mathbf{K}$ is the right- or left-propagation vector, and $\mathbf{r}$ is the position vector. In Eq. (4) E_o is the scalar amplitude in volts per meter of the electric field strength.

The phase and time-independent conjugate product

$$\Pi = \mathbf{E}_+^{(L)} \times \mathbf{E}_-^{(L)} = -\mathbf{E}_+^{(R)} \times \mathbf{E}_-^{(R)} = 2iE_o^2\mathbf{k} \tag{6}$$

is nonzero in a circularly polarized laser and is a purely complex quantity that is negative[22] to T and positive to P. It is a finite property of a circularly polarized laser that survives time averaging. It is, furthermore, an axial vector that is mathematically equivalent to an antisymmetric polar tensor Π_{ij}:

$$\Pi_i = \epsilon_{ijk}\Pi_{jk}, \tag{7}$$

where

$$\Pi_z = \begin{bmatrix} 0 & 2iE_o^2 & 0 \\ -2iE_o^2 & 0 & 0 \\ 0 & 0 & 0 \end{bmatrix}. \tag{8}$$

Here ϵ_{ijk} is the rank-three totally antisymmetric unit tensor.[5] Therefore Π_i is the complex antisymmetric part of the tensor product E_iE_j in Eq. (2).

In order to produce a real, scalar energy, Π_i must multiply a purely imaginary quantity of the same symmetry in the general product [Eq. (2)]. This quantity is the imaginary part of the complex dynamic electronic polarizability (α_{ij}), which from semiclassical theory[5] is the antisymmetric, T-negative, P-positive, second-rank, polar tensor

$$\alpha''_{\alpha\beta} = -\alpha''_{\beta\alpha} = -\frac{2}{\hbar}\sum_{j\neq n}\frac{\omega}{\omega_{jn}^2 - \omega^2}\,\mathrm{Im}(\langle n|\mu_\alpha|j\rangle\langle j|\mu_\beta|n\rangle). \tag{9}$$

Here $\mu_{\alpha,\beta}$ are electric dipole moment elements multiplying the quantum states n and j. The transition frequency between these states is

$$\omega_{jn} = \omega_j - \omega_n , \tag{10}$$

and the sum is over all states excluding the ground state n.[5,8,13] This polar tensor is mathematically equivalent to a T-negative, P-positive, rank-one axial vector through

$$\alpha_i'' = \epsilon_{ijk}\alpha_{jk}'' . \tag{11}$$

If the electromagnetic field is a circularly polarized pump laser propagating in axis Z of the laboratory frame, we have

$$\alpha_z'' = \alpha_{xy}'' - \alpha_{yx}'' \tag{12}$$

by definition of ϵ_{ijk} and from the theory of tensor products.

The required Hamiltonian is therefore conveniently written as

$$\Delta H_1 = (i/2)\alpha_i''\Pi_i , \tag{13}$$

which reduces to

$$\Delta H_1 = -\alpha_z''E_o^2 , \tag{14}$$

i.e., a simple product of the angular polarizability vector α_z'' and the square of the electric field strength of the pump laser. The latter can reach 10^9 V/m in a focused and Q-switched Nd:YAG laser, for example.

Note that in the optical Zeeman effect Π is the T-negative influence that activates the T-negative angular polarizability. Analogously, **B** activates the T-negative magnetic dipole moment m in the conventional Zeeman effect. This is of key importance in distinguishing the optical Zeeman effect from the optical Stark effect,[30] as is described in Section 3.

The interaction Hamiltonian [Eq. (14)] can be amplified greatly by tuning to resonance:

$$\omega \doteq \omega_{jn} , \tag{15}$$

i.e., by choosing a pump-laser frequency that is arbitrarily close to a natural transition frequency ω_{jn}. This technique is already well developed for the observation of the optical Stark effect,[33] which depends on the symmetric real part of the electronic polarizability. It should be a simple matter to adapt such an apparatus for the investigation of the optical Zeeman effect, for example, in a sodium atomic beam.[33] This possibility is considered further in Section 5.

3. COMPARISON WITH THE OPTICAL AUTLER-TOWNES (ac STARK) EFFECT

It is important to distinguish the optical Zeeman effect introduced here from the well-known effect first introduced by Autler and Townes[27] in 1955 and known as the ac, optical, or quadratic Stark effect. The latter was reviewed by Hanna *et al.*[30] and is described by an energy term proportional to the real part of the atomic or molecular electronic polarizability in Eq. (2.59) of Ref. 30, obtained from the first-order transition hyperpolarizability, Eq. (2.19) of Ref. 30. The real part of the electronic polarizability is defined in semiclassical theory[5] as a symmetric rank-two tensor, positive in motion reversal T,

$$\alpha'_{\alpha\beta} = \alpha'_{\beta\alpha} = \frac{2}{\hbar}\sum_{j\neq n}\frac{\omega_{jn}}{\omega_{jn}^2 - \omega^2}\,\mathrm{Re}(\langle n|\mu_\alpha|j\rangle\langle j|\mu_\beta|n\rangle) , \tag{16}$$

in the same notation as Eq. (9) of this paper. This tensor has no rank-one axial vector equivalent. The symmetry of the optical Stark effect is as different from that of the optical Zeeman effect, in consequence, as the conventional Stark effect is different from the conventional Zeeman effect.[37] These conventional effects are well known to be spectral splittings that are due, respectively, to static electric-field strength and static magnetic flux density. As with the conventional Stark and Zeeman effects, the spectral features of the optical (laser-induced) equivalents are entirely different from each other in general.

For example, the optical Stark effect has a nonvanishing zero-frequency component [when $\omega = 0$ in Eq. (16)], and the optical Zeeman effect does not [Eq. (9)]. The optical Stark effect can be observed experimentally[30] with lasers that are not circularly polarized, but the optical Zeeman effect vanishes if the pump laser is not circularly polarized, because the conjugate product Π vanishes from Eq. (6). Finally, and most important, the optical Zeeman effect is quantized (see Section 4) in the same way as angular momentum, permitting a rich variety of Clebsch–Gordan coupling of the electronic angular momentum **L**, the electronic spin angular momentum 2.002**S**, and the nuclear spin angular momentum **I**. This model is developed for a simple diatomic molecule in Section 4.

To observe the optical Zeeman effect, furthermore, it appears necessary only to make relatively minor changes in the apparatus already available for the optical Stark effect, primarily to ensure that the pump laser is completely circular polarized. A particularly sensitive method was described by Gray and Stroud[28]; other methods, using pump lasers that are not circularly polarized, were reviewed by Feneuille.[31] Whitley and Stroud[32] developed a comprehensive theory for the results obtained by Gray and Stroud,[28] using counterpropagating dye lasers orthogonal to a sodium atomic beam. Interestingly, Molander *et al.*[33] used circularly polarized radio-frequency and laser fields in the study of highly excited states of alkali metal atoms. Excitation of sodium atoms in an atomic beam was achieved up to the $n = 25$ manifold by dressing with a circularly polarized radio-frequency field at 200 MHz, with an electric-field strength of 8 V/cm maximum. The dressed state was then excited from the ground state with a resonant two-photon process by using a circularly polarized dye laser tuned exactly to resonance at 5890 Å with a sodium absorption. A second laser at 4115 Å excited the desired dressed state, the population of which flowed adiabatically into the circular orbit state after the radio-frequency state was turned off.

This method leaves 99% of the Rydberg population of the free sodium atoms in the aligned circular orbital state and can be adapted for the observation of the optical Zeeman splitting expected in the sodium atom from a coupling of **L** and **S** electronic angular-momentum quantum numbers in a Landé type Hamiltonian (Section 4). The effective angular polarizability in this method is greatly amplified by the precise tuning of a circularly polarized pump dye

laser to a natural absorption frequency of the sodium atomic beam. The optical Zeeman splitting would be measured by a tunable, unpolarized laser and would consist of characteristic patterns of several lines (Section 4), depending on the quantum numbers **L**, 2.002**S**, and **I** and on the intensity, frequency, and degree of circular polarity of the pump dye laser. The spacings of these lines give information about the electronic angular polarizability of free sodium atoms.

4. QUANTIZATION OF THE ANGULAR POLARIZABILITY: SELECTION RULES

The angular polarizability is a quantized axial vector with positive P and negative T symmetries, the same fundamental symmetries as quantized angular momentum. It can be seen that angular polarizability and angular momentum are proportional by using the interaction Hamiltonians

$$\Delta H_2 = -\gamma_e J_z B_z, \tag{17}$$

$$\Delta H_1 = -\alpha_z'' E_o^2, \tag{18}$$

where γ_e is the well-known gyromagnetic ratio linking the magnetic dipole moment m_i to the electronic orbital and spin angular momenta:

$$m_i = \gamma_e(\mathbf{L}_i + 2.002\mathbf{S}_i). \tag{19}$$

It follows that the angular polarizability itself can be written as

$$i\alpha_i'' = \gamma_\Pi(\mathbf{L}_i + 2.002\mathbf{S}_i), \tag{20}$$

where γ_Π is a gyroptic ratio between the optical conjugate product and the fundamental atomic or molecular angular momenta.

Therefore we have the important result that the spectral effects of the conjugate product Π can be developed theoretically in terms of the quantum theory of angular momentum, which in one form or another is the basis for much of quantum mechanics and spectroscopy.

One important practical consequence is that the conjugate product of a Nd:YAG or a dye laser can generate resonance effects akin to NMR and ESR, which are conventionally produced by magnetic flux density from a homogeneous magnet. The circularly polarized electromagnetic field can also be used to supplement **B** from an NMR or ESR magnet, for example, by circularly polarizing the megahertz- or gigahertz-frequency probes of these instruments. This will cause interesting Landé-type coupling and splitting of the NMR and ESR spectra and is discussed below in this section.

The symmetry of the angular polarizability in the molecule fixed frame is recorded in the literature's molecular point group character tables by the well-known R symbols, given usually in the last columns. The symmetry has the commutator properties of the angular momentum,

$$[\alpha_x'', \alpha_y''] = i\hbar\alpha_z'', \quad [\alpha_y'', \alpha_z''] = i\hbar\alpha_x'', \quad [\alpha_z'', \alpha_x''] = i\hbar\alpha_y'', \tag{21}$$

and is described by the angular-momentum quantum numbers, with the usual magnitude $[j(j+1)]^{1/2}$. It follows that all atomic or molecular sources of angular momentum contribute in general to the angular polarizability through the usual coupling models, for example, Hund, Clebsch–Gordan, Racah, and Griffith theories.[5,6] In general, therefore, the conjugate product Π causes spectral splitting of different kinds involving the various angular-momentum quantum numbers **L**, 2.002**S**, **I**, and the framework angular momentum **O**. This property gives a much richer spectrum, in theory, then does the optical Stark effect.

A particularly interesting possibility is the generation of nuclear and electronic resonance spectra through the hyperfine interactions of Π with 2.002**S** and **I**, leading to the optical equivalents of NMR and ESR. Orbital electronic resonance, for example, can be shown to occur to first order as follows.

The interaction Hamiltonian between α_z'' and Π_z can be considered in close analogy with a simple Hamiltonian,

$$\Delta H_3 = \gamma_N I_z B_z = -m_z^{(N)} B_z, \tag{22}$$

of NMR spectroscopy, where B_z is the magnetic flux density of the NMR magnet and $m_z^{(N)}$ is the nuclear magnetic dipole moment. Replacing the magnetically induced B_z in the Z axis by the circularly polarized pump laser and delivering Π_z in the Z axis, we have

$$\Delta H_4 = -\alpha_z'' E_o^2 = -\gamma_\Pi M_J E_o^2 \hbar, \tag{23}$$

$$M_J = J, J-1, \ldots, -J, \tag{24}$$

where M_J is the Z-axis component of the angular-momentum quantum number with selection rule

$$\Delta M_J = \pm 1. \tag{25}$$

If probe electromagnetic radiation of angular frequency ω_p in radians per second is directed at the atom or molecule being irradiated by Π_i of the pump laser, resonance occurs when

$$\omega_p = \gamma_\Pi E_o^2 \tag{26}$$

in the megahertz–gigahertz range for a pump-laser electric-field strength of 10^5–10^7 V/m, assuming a conservative order of magnitude[38] of 10^{-38} J^{-1} C^2 m^2 for the orbital polarizability. The angular polarizability can be amplified greatly by tuning the pump laser to a natural transition frequency ω_{jn} of Eq. (9), implying the need for a much lower pump electric-field strength.

To consider an example of the optical Zeeman effect in simple diatomics, we start with the Hamiltonian

$$\Delta H_4 = -\gamma_\Pi(\mathbf{L}_z + 2.002\mathbf{S}_z)E_o^2, \tag{27}$$

written in terms of the gyroptic ratio γ_Π and the fundamental electronic and spin angular-momentum quantum numbers. The selection rules for transitions between energy levels in the optical Zeeman effect, from Eqs. (23) and (27), are identical to those for the conventional Zeeman effect, given by

$$\Delta J = 0, \quad \Delta M_J = 0, \pm 1. \tag{28}$$

As in the conventional Zeeman effect,[37] a probe microwave field can be used to record the spectrum. When the pump and the probe fields are parallel, $\Delta M = 0$, giving

the π components of the optical Zeeman effect; when they are perpendicular, $\Delta M = \pm 1$, giving the σ components. In the optical Zeeman effect the static magnetic flux density of the conventional Zeeman effect is replaced by Π with, as we have seen, the same symmetry characteristics. The formal analogy between the two effects can be developed for diatomic molecules by following Chap. 11 of Ref. 39. The Hamiltonian, Eq. (27), is rewritten with the well-known Hund vector-coupling models. In the weak-coupling limit, **L** and 2.002**S** precess about the molecular axis, which in turn precesses about the total electronic angular momentum **J**. In the presence of Π **J** precesses about Π with projection M in the direction of Z. This allows the Hamiltonian [Eq. (27)] to be rewritten as

$$\Delta H_4 = -\frac{(\Lambda + 2.002\Omega)\gamma_\Pi M_z E_o^2}{J(J+1)}, \tag{29}$$

with Λ and Ω defined as

$$\Lambda = k_a \cdot \mathbf{L}, \qquad \Omega = k_a \cdot \mathbf{J}, \tag{30}$$

where k_a is a unit vector[39] in the axis of the diatomic (or linear molecule). As in the conventional Zeeman effect, this produces $2J + 1$ equally spaced laser Zeeman absorption lines corresponding to the possible values of M, the extent of the splitting being determined by the ratio of the interaction energy $\alpha_z'' E_o^2$ to the reduced Planck constant. Essentially speaking, the difference between the optical and conventional Zeeman effects can therefore be summarized through the fact that the former measures the gyroptic ratio γ_Π, and the latter the gyromagnetic ratio γ_e. In other words, the optical Zeeman effect is mediated by the angular polarizability and the conventional Zeeman effect by the magnetic dipole moment.

The analogy of Hund's case (b)[39] for the optical Zeeman effect is the Landé coupled Hamiltonian

$$\begin{aligned}\Delta H_4 = &-\frac{1}{2J(J+1)} \\ &\times \left\{ \Lambda^2 \frac{N(N+1) + S(S+1) - J(J+1)}{N(N+1)} \right. \\ &\left. + 2.002[J(J+1) + S(S+1) - N(N+1)] \right\} \\ &\times M_z \gamma_\Pi E_o^2,\end{aligned} \tag{31}$$

written in analogy with Eq. (11-5) of Ref. 39 for the conventional Zeeman effect. Equation (31) can be rewritten in terms of the Landé g_J factor

$$\Delta H_4 = -g_J M_z \gamma_\Pi E_o^2, \tag{32}$$

which is of the order of unity for molecules with a net electronic angular momentum, as in the conventional Zeeman effect. Otherwise ΔH_4 is dominated by the nuclear spin angular momentum **I**. In general, however, the g factor depends on the rotational angular momentum **J** and other angular momenta that may contribute to the optical Zeeman spectrum measured by the microwave probe and generated by the circularly polarized pump laser.

In the optical Zeeman effect, if the g factors in states J_1 and J_2, respectively, are g_1 and g_2, and if the transition frequency between J_1 and J_2 is ν_0, the spectrum will be a series of absorption lines defined by

$$\nu = \nu_0 + \frac{(g_2 - g_1) M_z \gamma_\Pi E_o^2}{\hbar} \tag{33}$$

for $\Delta M = 0$ (π components) and by

$$\nu = \nu_0 + \frac{[(g_2 - g_1) M_z \pm g_1]\gamma_\Pi E_o^2}{\hbar} \tag{34}$$

for $\Delta M = \pm 1$ (σ components), with M_2 the lower state. This spectral detail depends on the angular polarizability, which can be greatly amplified by tuning to resonance, as we have seen. In general the g factors of the optical Zeeman effect contain hyperfine contributions from the nuclear angular-momentum quantum number **I**, which cause NMR as mentioned above. This technique is conveniently referred to in this work as optical NMR and appears to be of considerable potential utility in the analytical laboratory both for atoms and molecules. Its electronic equivalent is optical ESR.

If the molecular structure is such that

$$g_1 = g_2, \tag{35}$$

then there is no π component of the optical Zeeman effect and there are only two frequencies in the σ component. In general there are several σ lines that can be observed with the microwave probe field with its electric component perpendicular to Π_z of the pump laser, so that the direction of propagation of the pump laser is parallel to the length, or broadest faces, of the microwave waveguide in the Z-axis of the laboratory frame. This orientation could be achieved, possibly, by incorporating the waveguide in the pump-laser cavity as in conventional infrared radio-frequency double resonance.[40,41] No optical Zeeman effect will be observed, however, if the pump laser is not circularly polarized.

The general appearance of the optical Zeeman effect is expected to be similar to that sketched for the conventional effect in Fig. 11-1 of Ref. 39 but will depend on the frequency as well as on the square of the electric-field strength of the pump laser. This dependence gives, in principle, a great deal of new information. Additionally, it is also possible to use a circularly polarized probe microwave field as discussed by Townes and Schawlow[39] and more recently by Molander *et al.*[33] in other contexts.

When hyperfine structure that is due to **I** is taken into account, the Hamiltonian [Eq. (32)] of the optical Zeeman effect must be modified to

$$\Delta H_5 = -g_J M_z \gamma_\Pi E_o^2 - g_I I_z \gamma_{\Pi n} E_o^2. \tag{36}$$

If the interaction energy represented by Eq. (36) is much smaller than the hyperfine energy, so that Π is deemed not to disturb the coupling between **J** and **I**, the vector-coupling model gives the new Landé-type Hamiltonian

$$\begin{aligned}\Delta H_5 = &-\{-\gamma_{\Pi n} g_I[I(I+1) + F(F+1) - J(J+1)] \\ &- \gamma_\Pi g_J[J(J+1) + F(F+1) - I(I+1)]\} \\ &\times \frac{M_F E_o^2}{2F(F+1)},\end{aligned} \tag{37}$$

where **F** is the total angular-momentum quantum number

and M_F is its projection onto the direction of Π_z, the laboratory frame Z axis. For a diamagnetic linear molecule both terms of the laser Zeeman effect described by Eq. (37) are roughly equal in magnitude, giving considerable extra spectral detail that can be used for analytical purposes in close formal analogy with conventional NMR spectroscopy.

5. DISCUSSION

Although the rich variety of spectral detail expected theoretically from the optical Zeeman effect, optical NMR, and optical ESR developed in this paper has not yet been observed experimentally, the first optical NMR results were presented at the 1991 St. Louis experimental NMR conference by Warren and co-workers,[42] who used only 1/2 W of laser power with a chiral sample. The circularly polarized laser was observed to induce shifts in the original methoxy and ring proton resonances of the order of magnitude of 1 Hz, at the instrumental limit. Further research[42] has eliminated artifacts caused by heating, and, without deuterium lock signals, definitive evidence has been gathered for the existence of optical NMR spectroscopy in a variety of samples. These and other experiments under way have demonstrated the feasibility of optical NMR as a significant new direction in spectroscopy and as an analytical technique. The mediating tensor in paramagnetic molecules and atoms in which there is a net electronic angular momentum is the antisymmetric, or vectorial, polarizability used in this first theory. For diamagnetics the mediating tensor is the magnetic electric electronic hyperpolarizability, β.

Theoretical investigations performed after this paper was submitted have shown the existence of Landé coupling and Fermi contact interaction between the laser-induced electronic angular momentum (mediated by either α or β or both in combination) and the nuclear spin angular momentum. In optical ESR the induced electronic angular momentum interacts with the permanent electronic set angular momentum.

Optical NMR and ESR effects are expected in atoms, for instance in the ground state of hydrogen, and in general the available theoretical understanding points toward several possible mechanisms in which the laser can affect the original NMR spectrum. The laser-induced magnetic dipole moment is directly proportional to the laser intensity in watts per unit area, and pulses of intense laser radiation are expected to produce commensurate optical NMR and optical ESR shifts. The theory also allows for splitting of the original resonances by the laser.

Here the optical Zeeman effect has been distinguished carefully in the theoretical arguments from the experimentally observed and well-known optical Stark effect. The bulk magnetization caused by circularly polarized pump laser has been observed experimentally[9,10] in low-temperature solids and room-temperature diamagnetic liquids by using a simple inductance coil and has become known as the inverse Faraday effect. It is interesting to compare the theory of the inverse Faraday and optical Zeeman effects through terms analogous to the A, B, and C coefficients first proposed by Serber[3] for the conventional Faraday and Zeeman effects. Serber's theory elegantly illustrates the link between magnetization, circular birefringence, and Zeeman splitting that is due to a magnetic field and can be analogously developed for use with intense circularly polarized pump lasers such as a dye laser, carbon dioxide laser, or a Q-switched Nd:YAG laser.

The semiclassical expression for the optical Zeeman effect can be developed as a Serber type A term in the following description of optical activity induced by a circularly polarized pump laser. The angle of rotation[3,5] that is due to the pump laser, measured by a plane-polarized probe, is

$$\Delta\Theta \doteq \frac{1}{2}\omega\mu_0 cl\frac{N}{d_n}E_o^2\sum_n\left[\langle\alpha''_{yxz}(f)\rangle + \frac{\langle\alpha''_z\alpha''_{xy}(f)\rangle}{kT}\right], \quad (38)$$

where ω is the angular frequency of the probe, μ_0 is the magnetic permeability in SI units, c is the velocity of light, l is the sample length in meters and N is the number of molecules per cubic meter and where $\langle\alpha''_{xyz}(f)\rangle$ is the weighted ensemble average[5,13-16] of a rank-three molecular property tensor defined through the Voigt–Born perturbation $\alpha''_{ijk}E_o^2$. The quantity f is the dispersive line shape function[5] of semiclassical theory, and kT is the thermal energy per molecule. Equation (38) can be rewritten in terms of Serber's A, B, and C terms as

$$\Delta\Theta = -\frac{\mu_0 clNE_o^2}{3\hbar}\left[\frac{2\omega_{jn}\omega^2}{\hbar}(f^2 - g^2)A + \omega^2 f\left(B + \frac{C}{kT}\right)\right], \quad (39)$$

where

$$A = \frac{3}{d_n}\sum_n(\alpha''_j - \alpha''_n)\mathrm{Im}(\langle n|\mu_x|j\rangle\langle j|\mu_y|n\rangle),$$

$$B = \frac{3}{d_n}\sum_n \mathrm{Im}\left\{\sum_{k\neq n}\left[\sum_{k\neq n}\frac{\langle k|\alpha''_z|n\rangle}{\hbar\omega_{kn}}(\langle n|\mu_x|j\rangle\langle j|\mu_y|k\rangle - \langle n|\mu_y|j\rangle\langle j|\mu_x|k\rangle) + \sum_{k\neq j}\frac{\langle j|\alpha''_z|k\rangle}{\hbar\omega_{kj}}(\langle n|\mu_x|j\rangle\langle k|\mu_y|n\rangle - \langle n|\mu_y|j\rangle\langle k|\mu_x|n\rangle)\right]\right\},$$

$$C = \frac{3}{d_n}\sum_n \alpha''_z\,\mathrm{Im}(\langle n|\mu_x|j\rangle\langle j|\mu_y|n\rangle).$$

These equations represent a sum over transitions from component states of a degenerate set to an excited state Ψ_j, which itself can be a member of a degenerate set of degeneracy d_n.

In this representation the optical Zeeman effect is the A term, expressed in terms of the angular polarizability in states n and j. The definition in state n is Eq. (16), and that in state j is

$$\alpha''_{\alpha\beta j} = -\alpha''_{\beta\alpha j} = -\frac{2}{\hbar}\sum_{k\neq j}\frac{\omega}{\omega_{kj}^2 - \omega^2}\mathrm{Im}(\langle j|\mu_\alpha|k\rangle\langle k|\mu_\beta|j\rangle), \quad (40)$$

where k is a state of higher energy than j. With the A, B, and C terms written in this way, weighted Boltzmann averaging has been used with the interaction energy

$$V(\Omega) = -\alpha''_z E_0^2. \quad (41)$$

When the circularly polarized pump laser is Q switched and simultaneously tuned to resonance, this energy can easily be of the order of kT itself at 300 K.

Note that in this description by the A term of the optical Zeeman effect a right circularly polarized pump laser delivers a photon with a $-\hbar$ projection in the Z axis, producing a change $\Delta M = -1$ in the atomic or molecular quantum state. In a left circularly polarized pump the photon is projected $\hbar$, and the selection rule is $\Delta M = 1$. In a linearly polarized pump the selection rule is $\Delta M = 0$, and there is no optical Zeeman effect. This case is accounted for classically in Eq. (6), in which the left conjugate product is positive and the right is negative. The sign change produced by switching the pump from left to right in the optical Zeeman effect is equivalent to reversing the direction of the magnetic field in the conventional Zeeman effect. As in the conventional effect, the A term that is due to Π of the optical Zeeman effect represents the splitting of lines by Π into right and left circularly polarized components. The magnetic dipole moment operator of the conventional effect is replaced by the angular polarizability of the optical effect.

6. COMPUTER SIMULATION AND SCIENTIFIC VISUALIZATION

The effect of a pulse of powerful circularly polarized laser radiation on an ensemble of chiral molecules was simulated by Evans and Wagnière[26] on the IBM ES/3090-600J supercomputer of the Cornell Theory Center and was visualized and animated, as reported here, by C. R. Pelkie of the Cornell National Supercomputer Facility (CNSF), a resource of the Cornell Theory Center, using both the supercomputer and IBM RISC System/6000 workstations. Data were generated on the supercomputer; scientific visualization was performed with software routines written at the CNSF, and more than 40,000 video images were created with commercial software running on the supercomputer and graphics workstations.

The animation is an intrinsic part of the argument presented in this paper for the imposition of angular momentum by a circularly polarized pump laser on the picosecond time scale. Specifically, the animation is of the S enantiomer of bromochlorofluoromethane and shows the statistical cross correlation[22] developed between components of the electric dipole vector. The resulting cross-correlation functions [26] are shown as time-lapsed scattergrams for various pump-laser electric-field strengths and angular frequencies. This kind of cross correlation is the fundamental dynamical signature describing the development of magnetization in the ensemble. In a chiral ensemble, such as that depicted in the animation, this magnetization is also accompanied by parity-conserving frequency-dependent electric polarization, which was described for the first time to our knowledge by Evans and Wagnière.[26] If such a polarization were observed in achiral ensembles, such as water, it would signal the presence of important and fundamental parity nonconserving spectral features.

The technique of field-applied molecular dynamics computer simulation relies on a simple but useful modification of the forces loop of a standard molecular dynamics algorithm (of any type) to add to the torque set up between an applied field of force and the appropriate molecular property, the arm. The technique was first introduced[42] for the interaction of a static electric field and a permanent electric dipole moment. Here the electric field is the force, and the dipole moment is the arm. In this context the technique yielded new insight into dielectric relaxation and its high-frequency adjunct the far infrared, rise and fall transients, decoupling effects, cross-correlation effects, and a variety of other phenomena summarized in Refs. 44 and 45. The technique was later extended to the interaction of circularly polarized radiation[46] with chiral and achiral molecular ensembles and produced new insights summarized in Ref. 47. In the case reported in Ref. 46 the arm was again a permanent dipole moment, but the externally applied field was the spinning electric field of a laser.

Evans and Wagnière[48] have begun a field-applied simulation of nonlinear-optical effects. In that case the arm is an induced dipole moment, which may be electric or magnetic. The induced dipole moment forms a torque that is set up between the induced electric dipole moment and the spinning electric component of the electromagnetic field. Further details of the algorithm and the torque are given in Ref. 48.

Molecular dynamics computer simulation is implemented with a modified forces loop; the torque is supplemented in this way by a component from the applied circularly polarized laser field. The field-applied simulation proceeds with 108–864 molecules, in general, with periodic boundary conditions and a time step of 0.005 ps, data being recorded every two time steps. The Cartesian components of the external torque are coded into the forces loop at an instant t, and the sample is allowed to regain equilibrium in the presence of the torque. This process involves several thousand time steps, which describe the rise transient and Langevin functions. Reequilibration takes place through a thermostating routine involving temperature rescaling (rotational and translational). This routine dissipates the rotational and translational kinetic energy generated by the applied torque. After completion of the reequilibration process, the sample is in field-on equilibrium, in which the molecular dynamics are investigated by animation. The sample is in a statistically stationary state, suitable for computation of time cross-correlation functions by time averaging over several thousand time steps. Time correlation functions are generated out to a maximum of 200 records separated by 0.01 ps. Most of these correlation functions are damped in ~200 records, so that running time averaging over several thousand time steps produces good statistics. A variety of correlation functions were computed and animated for both baseline (field-off) and field-applied conditions.

The phenomenon animated and analyzed statistically in this way is dynamic polarization,[48] which requires a chiral molecular framework and which illustrates one of the nonlinear-optical effects of a circularly polarized laser. Animation analysis dramatically revealed that a major influence of the laser is to spin the molecular angular-momentum vector about the propagation axis Z. This sets up cross-correlation functions between orthogonal Cartesian components; these functions can be analyzed with the statistical programs mentioned above. The animation proved to be an intrinsically useful research tool and revealed complex phenomena with great clarity.

The data generated by the simulation were used to create animations illustrating time-lagged cross correlations

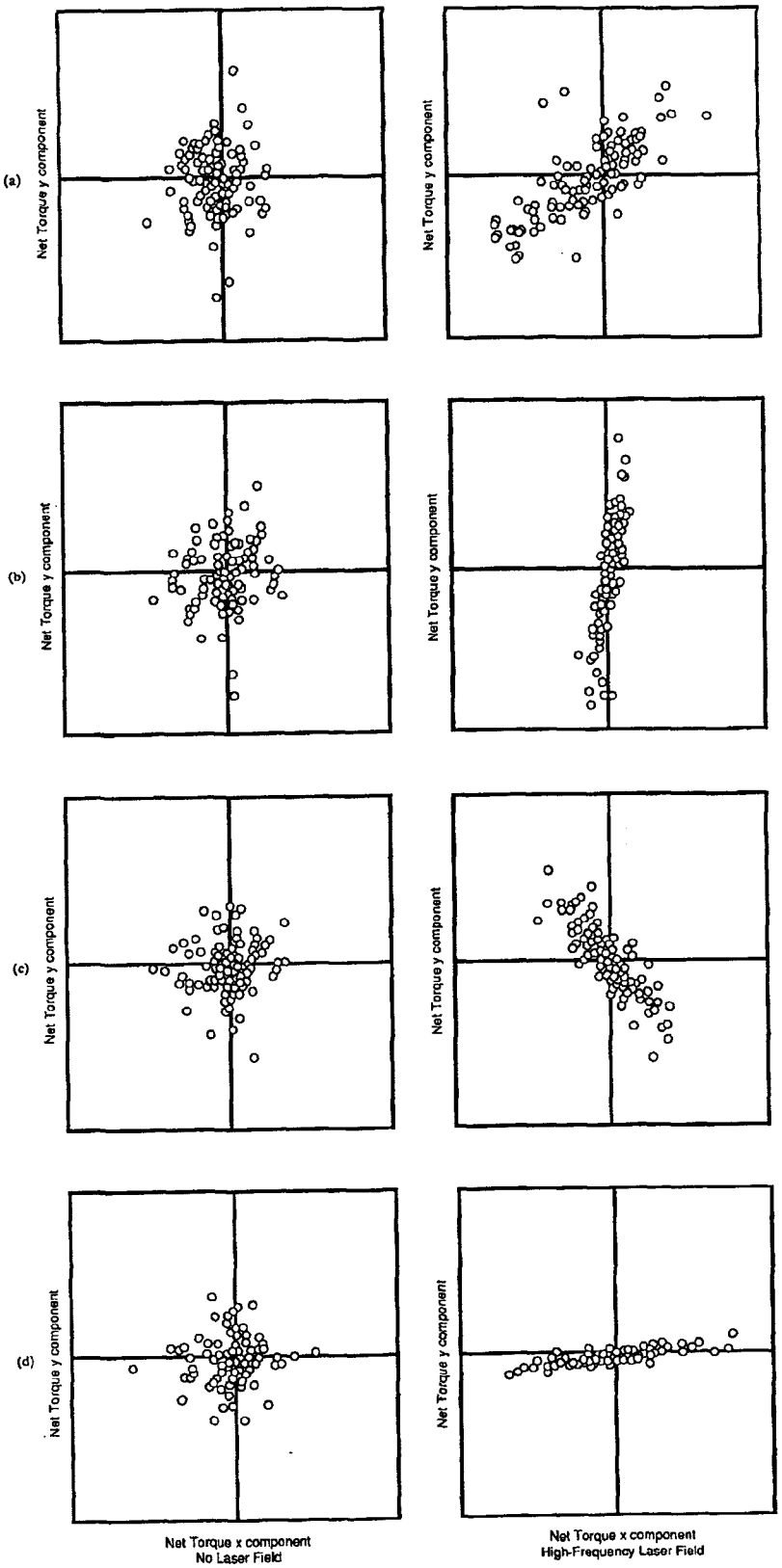

Fig. 1. Series of scattergrams measuring the net torque vectors with net torque y lagging net torque x by 0.08 ps at time t of (a) 0.01 ps, (b) 0.03 ps, (c) 0.05 ps, and (d) 0.07 ps in the simulation. (Thus net torque y is measured at time t + lag equal to 0.09, 0.11, 0.13, and 0.15 ps, respectively.) On the left in each image is shown the baseline condition (no laser, or field-off); the right-hand side illustrates the effect of a circularly polarized laser. The sequence clearly shows the motion of the field-on condition as a propellerlike movement of the ensemble scattergram, whereas in the baseline condition only random thermal motion is observed. Axes ranges are plus or minus the maximum net torque.

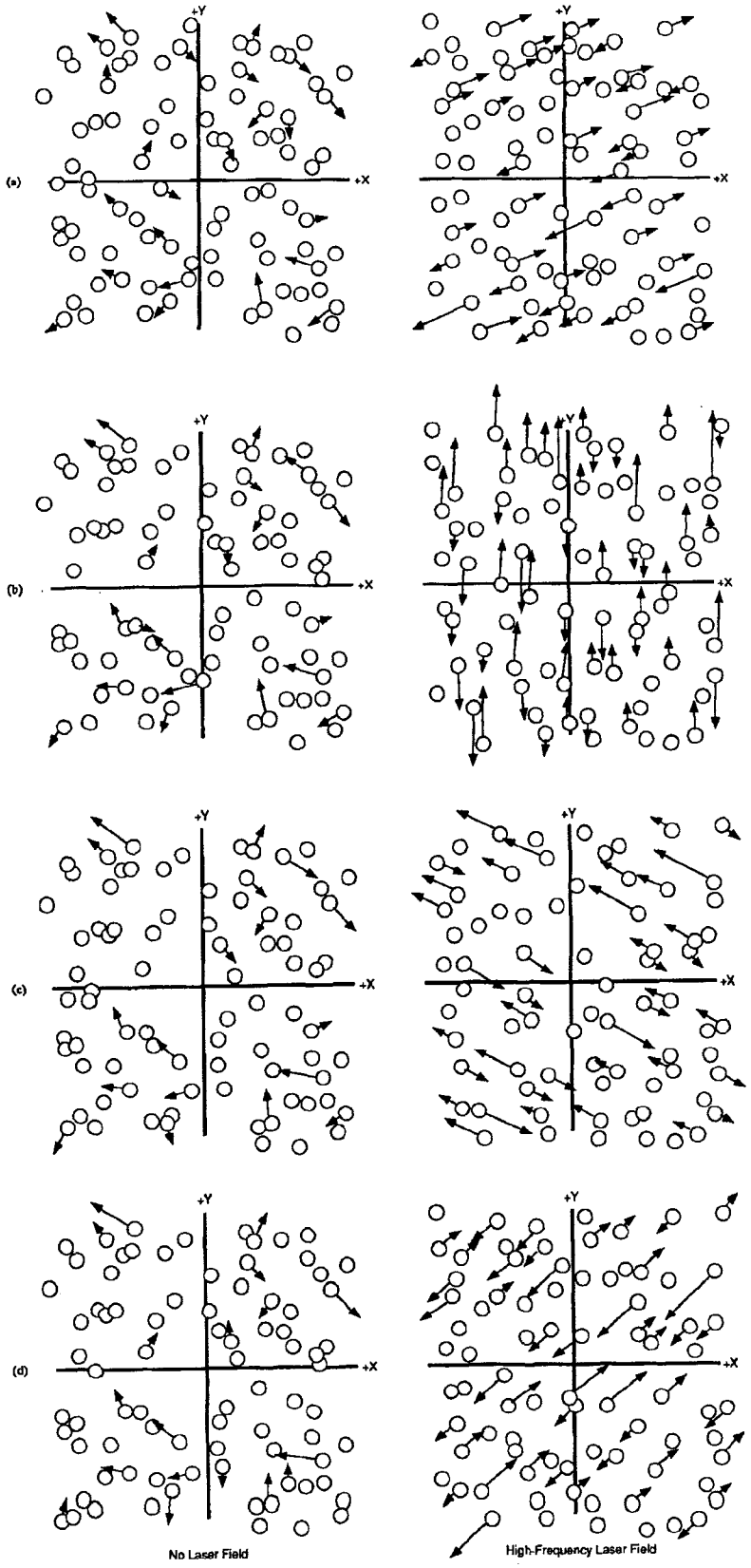

Fig. 2. Sequence of images of the ensemble's centers of molecular mass (circles) and net torque vectors (arrows). The laser is propagating directly into the ensemble on the right (down the Z axis, into the page); the left-hand ensemble shows the field-off condition. The torque vectors are rapidly rotated counterclockwise by the electromagnetic field's electric dipole vector. This sequence represents times (a) 1.51 ps, (b) 1.52 ps, (c) 1.53 ps, and (d) 1.54 ps, taken from the same simulation shown in Fig. 1. The Z axis is positive above the page, negative below.

between different vector components at selected lag times (Fig. 1). For each of the 108 molecules in the ensemble, the length of the x component of the selected vector (here, the net torque vector) was plotted as the horizontal deflection value of each point on the scattergram. The length of the y component of the same vector of the same molecule, measured at the later time (t + lag), was plotted as the vertical deflection of the scattergram point. Each animated scattergram sequence of 300 images represented 6 ps of simulated time. In another way of visualizing system behavior, molecular dynamics vectors (molecular angular momentum, net torque, net force, center of mass linear velocity, rotational velocity) were depicted as three-dimensional arrows originating at each molecular center of mass in the ensemble of molecules distributed in the cubic laboratory frame of reference. This technique dramatically revealed the highly correlated precession of the net torque vectors about the axis of laser propagation (Fig. 2). Similar behavior is observed for angular momentum, showing the physically important precessional effect of the laser on the angular momentum vectors of the ensemble, the precessional motion that gives rise to the effects of optical NMR.

7. CONCLUSIONS

The theory of optical NMR has been developed with reference to supercomputer simulation and animation. Optical NMR is produced by the conjugate product of a circularly polarized pump laser and is mediated by the angular polarizability, which is proportional to the angular-momentum quantum numbers through a new fundamental property called the gyroptic ratio. Optical NMR is accompanied by inverse Faraday magnetization, circular birefringence, and optical Zeeman splitting. These effects have been distinguished carefully from the optical or ac Stark effect.

ACKNOWLEDGMENTS

This research was conducted by using the Cornell National Supercomputer Facility, a resource of the Cornell Theory Center, which receives major funding from the National Science Foundation and IBM Corporation, with additional support from New York State and members of its Corporate Research Institute. The authors thank Malvin Kalos, Bruce Land, Wayne Lytle, Judy Warren, and Cynthia Harkleroad of the Cornell Theory Center and David Grossman of IBM for their assistance in this project.

A more detailed technical description of the animation process is available in our paper published in the *Proceedings of the 1990 IBM Supercomputing Competition*[49]; the paper and the animation received an Honorable Mention in the physical sciences division.

*Also with Material Research Laboratory, Pennsylvania State University, University Park, Pennsylvania 16802; address after August 1, Department of Physics, University of North Carolina, Charlotte, North Carolina 28223.

REFERENCES AND NOTES

1. M. Faraday, Philos. Mag. **28,** 294 (1846).
2. P. Zeeman, Philos. Mag. **43,** 236 (1896).
3. R. Serber, Phys. Rev. **41,** 489 (1932).
4. A. D. Buckingham and P. J. Stephens, Annu. Rev. Phys. Chem. **17,** 399 (1966).
5. L. D. Barron, *Molecular Light Scattering and Optical Activity* (Cambridge U. Press, Cambridge, 1982).
6. S. B. Piepho and P. N. Schatz, *Group Theory in Spectroscopy with Applications to Magnetic Circular Dichroism* (Wiley, New York, 1983).
7. P. S. Pershan, Phys. Rev. **130,** 919 (1963).
8. J. F. Ward, Rev. Mod. Phys. **37,** 1 (1965).
9. J. P. van der Ziel, P. S. Pershan, and L. D. Malmstrom, Phys. Rev. Lett. **15,** 190 (1965).
10. P. S. Pershan, J. P. van der Ziel, and L. D. Malmstrom, Phys. Rev. **143,** 574 (1966).
11. P. W. Atkins and M. H. Miller, Mol. Phys. **15,** 503 (1968).
12. Y. R. Shen, *The Principles of Non-Linear Optics* (Wiley, New York, 1984).
13. G. Wagnière, Phys. Rev. A **40,** 2437 (1989).
14. M. W. Evans, Phys. Rev. Lett. **64,** 2909 (1990).
15. M. W. Evans, Opt. Lett. **15,** 863 (1990).
16. M. W. Evans, Phys. Lett. A **146,** 485 (1990).
17. G. Wagnière and A. Meier, Chem. Phys. Lett. **93,** 78 (1982).
18. G. Wagnière and A. Meier, Experientia **39,** 1090 (1983).
19. G. Wagnière, Z. Naturforsch. Teil A **39,** 254 (1984).
20. L. D. Barron and J. Vrbancich, Mol. Phys. **51,** 715 (1984).
21. G. Wagniére, Z. Phys. D **8,** 229 (1988).
22. M. W. Evans, in *Advances in Chemical Physics,* I. Prigogine and S. A. Rice, eds. (Wiley Interscience, New York, 1991), Vol. 81, pp. 316 *ff.*
23. M. W. Evans, J. Mol. Spectrosc. **143,** 327 (1990).
24. M. W. Evans, Phys. Rev. A **41,** 4601 (1990).
25. M. W. Evans, J. Chem. Phys. **93,** 2329 (1990).
26. M. W. Evans and G. Wagnière, Phys. Rev. A. **42,** 6732 (1990).
27. S. H. Autler and C. H. Townes, Phys. Rev. **100,** 703 (1955).
28. H. R. Gray and C. R. Stroud, Opt. Commun. **25,** 359 (1978).
29. A. Schabert, R. Keil, and P. E. Toschek, Appl. Phys. **6,** 181 (1976).
30. D. C. Hanna, M. A. Yuratich, and D. Cotter, *Non-Linear Optics of Free Atoms and Molecules* (Springer, New York, 1979).
31. S. Feneuille, Rep. Prog. Phys. **40,** 1257 (1977).
32. R. M. Whitley and C. R. Stroud, Phys. Rev. A **14,** 1488 (1976).
33. W. A. Molander, C. R. Stroud, and J. A. Yeazell, J. Phys. B **19,** 1461 (1986).
34. M. W. Evans, J. Mod. Opt. **37,** 1655 (1990).
35. W. M. Evans, Spectrochim. Acta **46A,** 1475 (1990).
36. L. D. Barron and C. G. Gray, J. Phys. A **6,** 59 (1973).
37. P. W. Atkins, *Molecular Quantum Mechanics* (Oxford U. Press, Oxford, 1983).
38. S. Kielich, in M. Davies (senior reporter), *Dielectric and Related Molecular Processes,* Vol. 1 of Chemical Society Specialist Periodical Reports (Chemical Society, London, 1972), p. 151.
39. C. H. Townes and A. L. Schawlow, *Microwave Spectroscopy* (McGraw-Hill, New York, 1955; reprinted by Dover, New York, 1975), Chap. 11.
40. E. Arimondo, P. Glorieux, and T. Oka, Phys. Rev. A **17,** 1375 (1978).
41. Ch. Salomon, Ch. Breant, A. van Leberghe, G. Camy, and C. U. Bordé, Appl. Phys. B **29,** 153 (1982).
42. W. S. Warren, S. Mayr, D. Goswami, and A. P. West, Jr., Science **255,** 1683 (1992).
43. M. W. Evans, J. Chem. Phys. **76,** 5473, 5480 (1982).
44. M. W. Evans, P. Grigolini, G. Pastori, I. Prigogine, and S. A. Rice, eds., *Advances in Chemical Physics* (Wiley Interscience, New York, 1985), Vol. 62, Chap. 5.
45. Ref. 44, Vol. 63, Chap. 4.
46. M. W. Evans, G. C. Lie, and E. Clementi, J. Chem. Phys. **87,** 6040 (1987).
47. M. W. Evans, in *Advances in Chemical Physics,* I. Prigogine and S. A. Rice, eds. (Wiley Interscience, New York, 1991), Vol. 81; this ~400-page review lists ~450 references.
48. M. W. Evans and G. Wagnière, Phys. Rev. A **42,** 6732 (1990).
49. M. W. Evans and C. R. Pelkie, "Scientific excellence in supercomputing," in *Proceedings of the 1990 IBM Supercomputing Competition* (Baldwin, Athens, Ga., 1992).